The Spine Journal 18 (2018) 1222–1230

Basic Science

Load-sharing through elastic micro-motion accelerates bone formation and interbody fusion

Eric H. Ledet, PhD[a,b,c,*], Glenn P. Sanders, PhD[a], Darryl J. DiRisio, MD[a,d], Joseph C. Glennon, VMD[e]

[a]*ReVivo Medical, 33 Old Niskayuna Rd, Loudonville, NY 12211, USA*
[b]*Department of Biomedical Engineering, Rensselaer Polytechnic Institute, 110 8th St, Troy, NY 12180, USA*
[c]*R&D Service, Stratton VA Medical Center, 113 Holland Ave, Albany, NY, 12208, USA*
[d]*Department of Neurosurgery, Albany Medical College, 47 New Scotland Ave, Albany, NY 12208, USA*
[e]*Veterinary Specialties Referral Center, 1641 Main St, Pattersonville, NY 12137, USA*

Received 8 September 2017; revised 6 January 2018; accepted 1 February 2018

Abstract

BACKGROUND CONTEXT: Achieving a successful spinal fusion requires the proper biological and biomechanical environment. Optimizing load-sharing in the interbody space can enhance bone formation. For anterior cervical discectomy and fusion (ACDF), loading and motion are largely dictated by the stiffness of the plate, which can facilitate a balance between stability and load-sharing. The advantages of load-sharing may be substantial for patients with comorbidities and in multilevel procedures where pseudarthrosis rates are significant.

PURPOSE: We aimed to evaluate the efficacy of a novel elastically deformable, continuously load-sharing anterior cervical spinal plate for promotion of bone formation and interbody fusion relative to a translationally dynamic plate.

STUDY DESIGN/SETTING: An in vivo animal model was used to evaluate the effects of an elastically deformable spinal plate on bone formation and spine fusion.

METHODS: Fourteen goats underwent an ACDF and received either a translationally dynamic or elastically deformable plate. Animals were followed up until 18 weeks and were evaluated by plain x-ray, computed tomography scan, and undecalcified histology to evaluate the rate and quality of bone formation and interbody fusion.

RESULTS: Animals treated with the elastically deformable plate demonstrated statistically significantly superior early bone formation relative to the translationally dynamic plate. Trends in the data from 8 to 18 weeks postoperatively suggest that the elastically deformable implant enhanced bony bridging and fusion, but these enhancements were not statistically significant.

CONCLUSIONS: Load-sharing through elastic micro-motion accelerates bone formation in the challenging goat ACDF model. The elastically deformable implant used in this study may promote early bony bridging and increased rates of fusion, but future studies will be necessary to comprehensively characterize the advantages of load-sharing through micro-motion.

Keywords: Anterior; Cervical; Fusion; Load-sharing; Micro-motion; Plate

FDA device/drug status: Investigational (ReVeal Anterior Cervical Plate); Approved (Swift Anterior Cervical Plate).

Author disclosures: ***EHL:*** Grant: NIAMS of NIH (F, Paid directly to institution/employer), pertaining to the submitted work; Private Investments: ReVivo Medical (21%); Board of Directors: ReVivo Medical (None), outside the submitted work. ***GPS:*** Grant: NIAMS of NIH (F, Paid directly to institution/employer), pertaining to the submitted work; Private Investments: ReVivo Medical (20%); Board of Directors: ReVivo Medical (None), outside the submitted work. ***DJD:*** Grant: NIAMS of NIH (F, Paid directly to institution/employer), pertaining to the submitted work; Private Investments: ReVivo Medical (25%); Board of Directors: ReVivo Medical (None), outside the submitted work. ***JCG:*** Stock Ownership: ReVivo Medical (1%); outside the submitted work.

The disclosure key can be found on the Table of Contents and at www.TheSpineJournalOnline.com.

* Corresponding author. ReVivo Medical, 33 Old Niskayuna Rd, Loudonville, NY 12211, USA. Tel.: (518) 227-0743; fax: (518) 262-5400; Department of Biomedical Engineering, Rensselaer Polytechnic Institute, 110 8th St, JEC 7044, Troy, NY 12180; Research and Development Service, Stratton VA Medical Center, 113 Holland Ave, Albany, NY 12208.

E-mail address: eledet@revivomedical.com (E.H. Ledet)

https://doi.org/10.1016/j.spinee.2018.02.004

Background

Success rates for one- and two-level anterior cervical discectomy and fusion (ACDF) procedures are high, but outcomes are not as good for patients with diabetes, chronic obstructive pulmonary disease, osteoporosis, and patients with nicotine exposure or exposure to medications that hinder bone formation (steroids, proton pump inhibitors, etc.) [1–5]. Likewise, in patients where three or more motion segments must be included in the fusion construct, most surgeons choose to do a combined anterior and posterior reconstruction, as fusion rates are reduced in these situations and construct failure is high with an anterior alone approach [6,7].

Achieving a successful spinal fusion requires the proper biological and biomechanical environment. By Wolff's Law [8], bone formation is stimulated by mechanical loading, but if the loading is excessive, high strains or unwanted motion can lead to fibrous tissue formation [9–11].

Seminal research in fracture fixation biomechanics has demonstrated that rigid fixation (<2% strain) leads to primary bone formation [12], less rigid fixation (2%–10% strain) leads to secondary bone formation [13], and more compliant fixation (>10% strain) results in fibrous non-union. The current designs of fracture fixation plates, intramedullary rods, and external fixation systems are based on these guiding biomechanical principles.

The goals of spinal fusion and fracture fixation are fundamentally the same—facilitate bone growth—and so it is intuitive that the biomechanics of spine fusion is quantitatively similar to fracture healing. Following arthrodesis, the extent of loading and motion is largely dictated by the properties of the implants used to stabilize the spine. The ideal cervical plate stabilizes a motion segment sufficiently to facilitate bone formation and at the same time fosters load-sharing and eliminates stress-shielding [14]. The ideal cervical plate also allows long-term loading through the fusion mass to facilitate maturation of the bone.

Plate stiffness is key to performance [15–18]. There is a correlation between implant stiffness, instantaneous axis of rotation, and interbody loading [15,16]. If too rigid, the plate will stress-shield, reverse-load the graft, and have a high likelihood of causing subsidence and graft failure or screw loosening [19–22]. If too flexible, excess motion between the graft and end plates will favor pseudarthrosis over fusion [23].

Current static plates are rigid and do not load-share. They unload the graft and stress-shield in flexion [17,24] and overload in extension [19]. Dynamic plates allow for load-sharing only over a limited range of motion. Translationally dynamic designs are composed of sliding mechanisms with hard stops. When sliding, the plates bear minimal load and they allow all of the forces to be transmitted through to the graft. This can lead to graft subsidence [25]. Then, when the range of motion reaches the limit of the sliding range, the sliding mechanism hits a hard stop, there is an abrupt change in the mechanics, and dynamic plates effectively become static plates.

Fig. 1. The one-level 24-mm elastically deformable plates used in this study were fabricated from titanium alloy and were designed to allow controlled micro-motion during physiological loading.

The stiffness of the plate largely dictates the biomechanics experienced by the graft [26]. Ideally, the plate affords a balance somewhere between overloading (and excessive motion) and underloading (and stress shielding). To facilitate controlled continuous load-sharing with the interbody space, we evaluated an elastically deformable anterior cervical plate which promotes load-sharing through controlled micro-motion (ReVeal Anterior Cervical Plating System, ReVivo Medical, Loudonville, NY, USA) (Fig. 1). Under the full range of physiological loading, the plate continuously deforms elastically, promoting load-sharing with the interbody space.

The purpose of this study was to evaluate the efficacy of the elastically deformable, continuously load-sharing spinal plate to promote faster and higher quality spinal fusion relative to an existing translationally dynamic plate in vivo in an animal model of ACDF.

Materials and methods

Implants

The elastically deformable plate design is analogous to a serpentine spring with double struts supporting each transverse member of the spring. The properties of the transverse members and struts are designed to stabilize the motion

segment to facilitate interbody fusion while also promoting a favorable load-sharing environment with the interbody space through the entire range of physiological motion. The mechanical properties foster elastic micro-motion and load-sharing with the cage or graft. The elastically deformable plates are monolithic (comprising a single component) and were fabricated from titanium alloy (Ti-6Al-4V) using traditional computer numerical control machining techniques (Lowell, Inc, Brooklyn Park, MN, USA).

Animals

Fourteen castrated, dehorned, male, skeletally mature, Alpine-Nubian cross-bred goats (Noble Life Sciences, Sykesville, MD, USA) were used in the study. Animals underwent standard screening procedures, including biplanar plain radiographs of the cervical spine. For the duration of the study, animals were singly housed in pens.

Surgery

After Institutional Animal Care and Use Committee approval, an ACDF was performed on each goat, with animals grouped to receive either a single-level 24-mm anterior dynamic plate (n=6) or a single-level 24-mm anterior elastically deformable plate (n=8).

Each animal was positioned supine with the head and neck hyperextended. Under general anesthesia and using standard aseptic techniques, an incision was made parallel and medial to the sternocleidomastoid muscle. The muscles and soft tissue were dissected bluntly and a ventral approach was made to expose the C34 intervertebral disc space of all animals (except one animal where C45 was exposed). A single-level discectomy was performed and a polyether ether ketone (PEEK) interbody cage (8-mm height) was filled with local autograft from the vertebral body. (There is a ventral ridge on the superior vertebra which was removed with rongeurs to gain access to the disc space. The corticocancellous bone from that ridge was used to fill the cage.) The interbody cage was then gently impacted into the disc space. After the cage was placed, the animal was then randomly assigned to either the dynamic or the elastically deformable treatment group. In each case, the plate was affixed to the C3 and C4 vertebra (C4 and C5 in one animal) in standard clinical fashion with two screws per vertebra (Fig. 2). All dynamic plates were fixed with 20 mm long 4.25-mm φ screws and elastically deformable plates with 4.0-mm φ screws. The manufacturer's recommended screws and techniques were used for each plate. For the translationally dynamic plate, the plate incorporates self-locking bushings that lock the screws to the plate. The elastically deformable plate incorporates anti-backout (but not locking) features to prevent the screws from backing out. Following cage and plate placement, the wound was irrigated and meticulously closed in layers with non-absorbable sutures followed by surgical staples to close the skin.

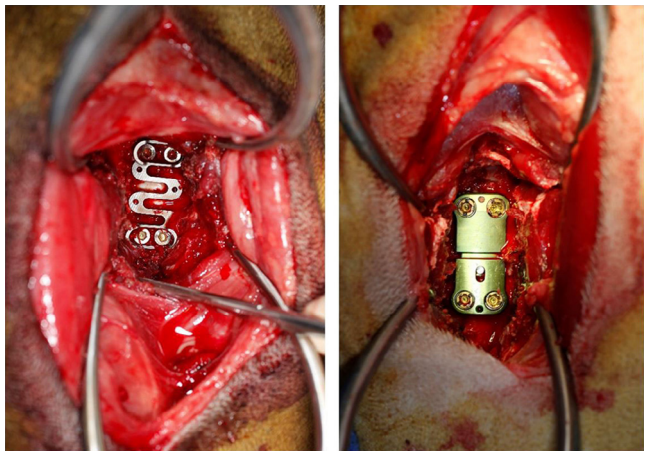

Fig. 2. Single-level 24-mm elastically deformable plates (Left) and dynamic plates (Right) were placed using standard ACDF techniques with a PEEK interbody cage filled with local autograft. ACDF, anterior cervical discectomy and fusion; PEEK, polyether ether ketone.

X-ray studies

Immediately postoperatively and at 2 and 6 weeks postoperatively, each animal had lateral and dorsal-ventral plain radiographs taken of cervical spine while animals were awake and in neutral position. Plain radiographs were used to confirm postoperative positioning of implants and at 2 and 6 weeks were assessed for gross changes in implant or screw position, loss of fixation, etc.

Computed tomography (CT) scans

At 8 and 12 weeks postoperatively, animals were anesthetized and the cervical spine was CT scanned. Axial images of 0.5-mm thickness with 0.5-mm overlap were acquired. Images were reconstructed and used to quantify extent of new bone formation and bridging bone, and to assess hardware changes (screw backout and implant migration).

At both time points (8 and 12 weeks), a six-point scale was used to quantify bridging bone by assessing formation of bone that spanned from end plate to end plate in the anterior zone, posterior zone, left lateral zone, right lateral zone, within zone, and peripheral zone [27,28]. The "within zone" comprises the area inside of the cage and the "peripheral zone" comprises the extradiscal space including facet joints.

An independent musculoskeletal radiologist reviewed and assessed axial images and coronal and sagittal reconstructions at both time points. To minimize any potential bias in qualitative evaluation of images, the radiologist was blinded to the goals of the study, the overall study design, the time points of the CT scans, and details of the treatment groups. The radiologist was only provided with the scans and the rubric for grading. No attempt was made to obscure the plate on the scans because doing so may have inadvertently obscured features of the healing (ie, bone growing in, through, or around the plate).

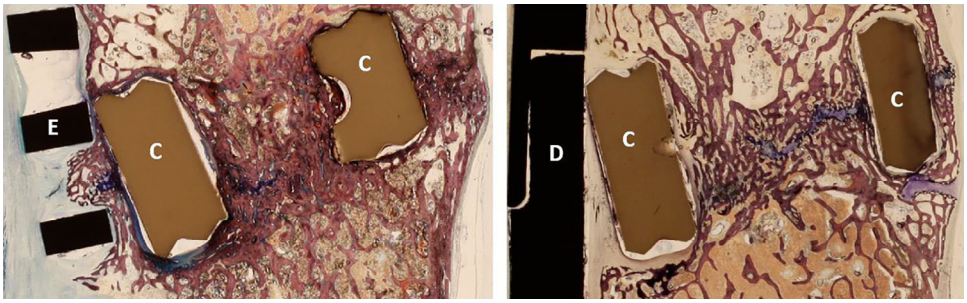

Fig. 3. Mid-sagittal sections were used to quantify the volume of bone filling the PEEK interbody cage. The fraction of bone filling the cage was compared between the elastically deformable plate group (Left) (Animal 108) and the dynamic plate group (Right) (Animal 106). Sections are stained with Stevenel's Blue and Van Gieson Picro Fuchsin. C, cage; D, dynamic plate; E, elastically deformable plate; PEEK, polyether ether ketone.

The extent of bone formation within the interbody space was assessed, and motion segments were classified as follows:

1. Definitely not fused: Little evidence of new bone formation (non-bridging).
2. Probably not fused: Evidence of some bone formation but less than half the volume of the interbody cage and non-bridging.
3. Possibly not fused: Evidence of bone formation filling the cage but non-bridging.
4. Possibly fused: Bridging bone from end plate to end plate in at least one image (but less than half the volume of the interbody cage).
5. Probably fused: Bridging bone filling more than half of the volume of the interbody cage.
6. Definitely fused: Bridging bone filling the volume of the cage.

Euthanasia and necropsy

At the end of the study period (n=3 at 14 weeks for dynamic plate, n=5 at 14 weeks for elastically deformable plate, n=3 at 18 weeks for dynamic plate, n=3 at 18 weeks for elastically deformable plate), animals were euthanized, the cervical spine was harvested en bloc, and the instrumented motion segment was isolated for post mortem analyses. Specimens were then placed in 10% neutral buffered formalin for undecalcified histologic evaluation.

Undecalcified histology

Specimens were routinely processed undecalcified and embedded in methyl methacrylate (Alizée Pathology, Thurmont, MD, USA). Longitudinal sections were prepared parallel to the sagittal plane and stained with Stevenel's Blue and Van Gieson Picro Fuchsin for analysis. Sections were examined qualitatively for the appearance of new bone, fibrous tissue, and inflammation.

To quantify the amount of bone that had formed in the interbody space, scanning micrographs of the interbody cage (Fig. 3) were taken from the mid-sagittal sections and examined quantitatively using image analysis (ImageJ, NIH). The bone fraction filling the space within the cage was measured by defining a region of interest within the cage. Bone tissue was selectively thresholded and then quantified as shown in Fig. 4. The area of tissue was then normalized to the total area of the cage and expressed as an area fraction.

Data analysis

From CT scans, categorical values (bridging zones and fusion status) were compared between treatment groups using a Mann-Whitney or Fisher exact test. Mean values of bone area fraction from histology were compared using an independent means *t* test. Values were deemed statistically significant for $p \leq .05$. All statistical analyses were conducted using SPSS (IBM Analytics, Armonk, NY, USA).

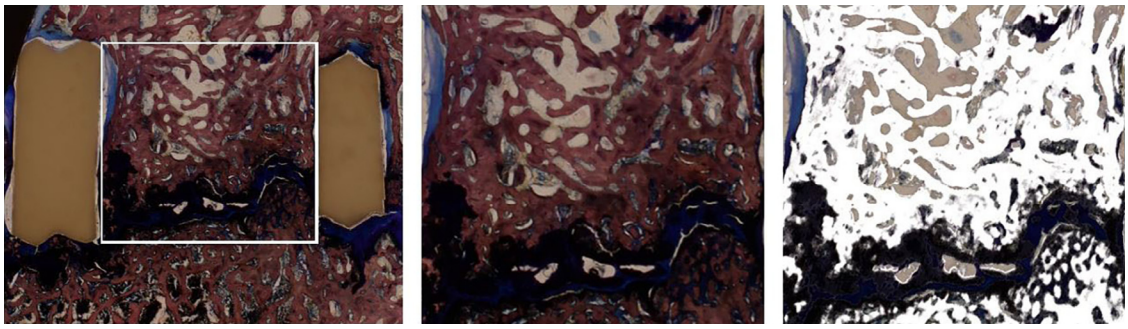

Fig. 4. To quantify bone formation in the interbody space, a region of interest was selected within the interbody cage (left and center). Bone tissue was selectively thresholded (Right), quantified, and expressed as a fraction of the total area of the region of interest.

Results

Surgery

Eight animals received the elastically deformable plate and six animals received the dynamic cervical plate. One animal in the elastically deformable group and one animal in the dynamic group exhibited transient foreleg paraparesis postoperatively, likely due to a screw in each case which penetrated the posterior cortex of the C3 vertebra. The neurologic deficit in both animals resolved, and there were no other intraoperative or postoperative complications.

X-ray studies

Plain radiographs showed satisfactory placement of all implants (Fig. 5). At 2 weeks, there was evidence of minimal ventral migration of the caudal end of the plate in one animal in the dynamic group (103) and the cranial end of the plate in one animal in the elastically deformable group (108). There was no evidence of cage migration and no screws or plates backed out of the vertebrae at any time points. There were no other hardware-related issues.

CT scans

CT scans demonstrated progressive new bone formation in all animals by 8 weeks. At both 8 and 12 weeks, there was a spectrum in the extent of bone formation and bridging bone (Fig. 6). Some animals demonstrated minimal new bone formation, some demonstrated significant bone formation that was non-bridging, and some animals demonstrated substantial bridging bone.

At 8 weeks, 62.5% (5/8) of animals in the elastically deformable group were either probably fused or definitely fused compared with 16.7% (1/6) of animals in the dynamic group. These differences were not statistically significant (p=.121), which is likely due to the small sample size (power=0.55, effect size 0.89, minimum detectible difference between treatment groups 86%). Importantly, at 8 weeks, only one animal (12.5%) in the elastically deformable group was possibly not fused (and no animals were worse than possibly not fused), whereas in the dynamic group at 8 weeks, there were four animals (66.7%) that were probably not fused.

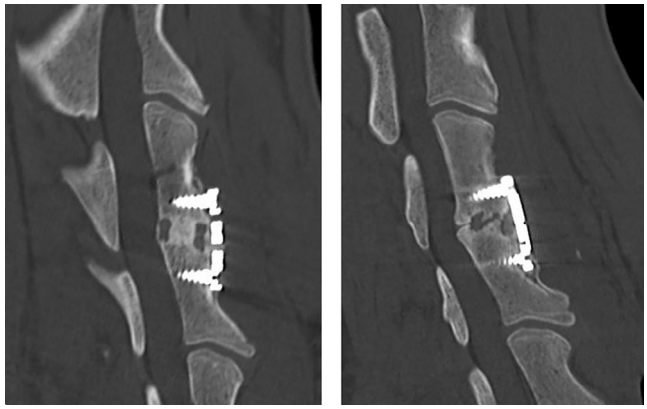

Fig. 6. Based on CT scan, extent of bone formation and bridging was variable among animals and treatment groups ranging from robust bridging bone (Left) (Animal 310 at 12 weeks) to some bone formation without bridging (Right) (Animal 301 at 12 weeks). CT, computed tomography.

By 12 weeks, 6 of 8 animals (75%) in the elastically deformable group were either probably fused or definitely fused compared with 2 of 6 animals (33.3%) in the dynamic group. These differences were not statistically significant (p=.156), also likely due to the small sample size (power=0.46, effect size 0.81, minimum detectible difference 85%). Quantitative assessment of bridging and fusion status is shown in Figs. 7 and 8 and Table 1. At both time points, the elastically deformable group demonstrated a higher number of fusions and lower number of protracted fusions than the dynamic plate group, but these differences were not statistically significantly.

At both 8 and 12 weeks, there was evidence of bridging bone in many animals. As expected, the earliest bridging bone was generally within the interbody cage. The mean number of zones bridged in elastically deformable treated animals was

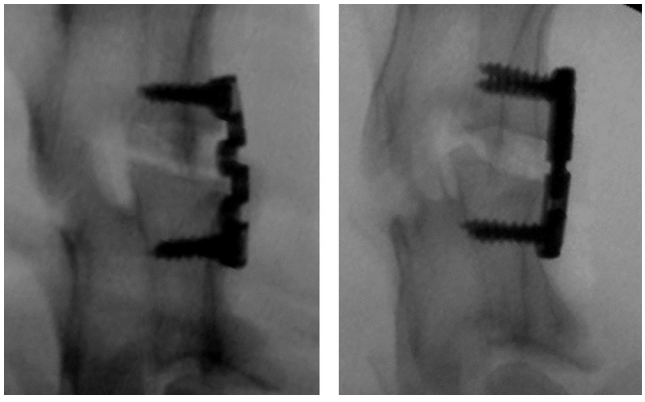

Fig. 5. Lateral plain x-rays were taken postoperatively and at 2 and 6 weeks postoperatively of elastically deformable plate-treated motion segments (Left) and dynamic plate-treated motion segments (Right).

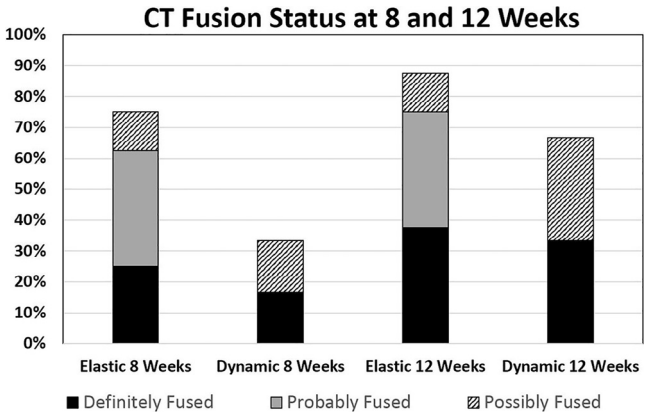

Fig. 7. Based on CT scans at 8 weeks and 12 weeks, treated levels were classified as definitely fused, probably fused, possibly fused, possibly not fused, probably not fused, or definitely not fused. CT, computed tomography.

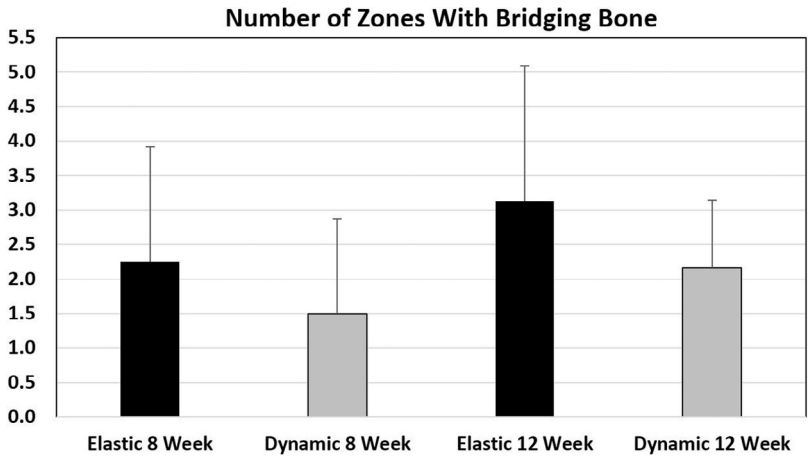

Fig. 8. Bridging bone was assessed from CT scans at 8 weeks and 12 weeks. Treated levels were assessed for bridging in the anterior, posterior, left lateral, right lateral, within, and peripheral zones. CT, computed tomography.

greater than dynamic plated animals at both 8 and 12 weeks. Quantitative analysis of bridging zones indicated a mean of 2.25 zones bridged in elastically deformable animals at 8 weeks compared with 1.50 zones bridged in dynamic-plated animals. This increase was not statistically significant (p=.573, power=0.59, effect size 0.49, minimum detectible difference 2.5). At 12 weeks, there was a mean of 3.13 zones bridged in elastically deformable animals and 2.17 zones in dynamic-plated animals. This increase was not statistically significant (p=.491, power=0.20, effect size 0.59, minimum detectible difference 2.7). Quantitative assessment of bridging and fusion status is shown in Table 1.

Undecalcified histology

Histology was consistent with CT scans. All specimens demonstrated new bone formation, and, similar to CT scans, there was a spectrum in the extent of bone formation and bridging bone. The most exuberant response was within the interbody cage in all animals.

There was well developed fibrous encapsulation of the PEEK cages in all animals, consistent with a normal chronic foreign body response. There was focal evidence of PEEK fragments in some specimens, likely residual from the surgical procedure. There was no inflammatory or foreign body

Table 1
Quantitative assessment of bridging and fusion status

Animal ID	Tx group	Fusion status 8 weeks	Fusion score* 8 weeks	Bridging zones 8 weeks	Fusion status 12 weeks	Fusion score* 12 weeks	Bridging zones 12 weeks
101	Elastic	Definitely fused	6	2	Definitely fused	6	3
102	Elastic	Definitely not fused	1	2	Probably fused	5	5
104	Elastic	Probably fused	5	2	Possibly not fused	3	2
105	Elastic	Possibly fused	4	1	Probably fused	5	1
108	Elastic	Probably fused	5	6	Definitely fused	6	6
306	Elastic	Probably fused	5	1	Probably fused	5	1
308	Elastic	Possibly not fused	3	1	Possibly fused	4	2
310	Elastic	Definitely fused	6	3	Definitely fused	6	5
		Mean (St dev)	**4.38** (1.69)	**2.25** (1.67)	**Mean** (St dev)	**5.00** (1.07)	**3.13** (1.96)
103	Dynamic	Probably not fused	2	3	Definitely fused	6	3
106	Dynamic	Possibly fused	4	3	Possibly fused	4	3
107	Dynamic	Probably not fused	2	1	Possibly fused	4	1
301	Dynamic	Probably not fused	2	0	Probably not fused	2	1
309	Dynamic	Probably not fused	2	0	Probably not fused	2	2
312	Dynamic	Definitely fused	6	2	Definitely fused	6	3
		Mean (St dev)	**3.00** (1.67)	**1.50** (1.38)	**Mean** (St dev)	**4.00** (1.79)	**2.17** (0.98)

St dev, standard deviation.

* Fusion score: (6) Bridging bone filling cage. (5) Bridging bone filling more than half of the cage. (4) Bridging bone in at least one location in (but less than half of) the cage. (3) Bone filling cage but non-bridging. (2) Some bone (half or less) in cage (non-bridging). (1) Little evidence of new bone (non-bridging).

Table 2
Quantitative analysis of bone filling the interbody cage

Animal ID	Tx group	Time point (weeks)	% Area in cage filled with bone
101	Elastic	14	62.1
102	Elastic	14	56.5
104	Elastic	14	51.7
105	Elastic	14	59.8
108	Elastic	14	65.2
		Mean (St dev)	**59.1** (5.2)
103	Dynamic	14	43.1
106	Dynamic	14	43.2
107	Dynamic	14	47.6
		Mean (St dev)	**44.63** (2.1)
306	Elastic	18	35.0
308	Elastic	18	35.4
310	Elastic	18	53.3
		Mean (St dev)	**41.2** (8.5)
301	Dynamic	18	14.8
309	Dynamic	18	21.5
312	Dynamic	18	43.7
		Mean (St dev)	**26.7** (12.4)

St dev, standard deviation.

response to any of the screws or plates, and in all animals there was good osseointegration of the screws in the vertebral bodies and no evidence of fibrous tissue formation around the screws. There was no evidence of acute inflammation or particulate debris in any specimen. In all elastically deformable levels, there was some new bone formation extending from the anterior vertebral body to the space between the "rungs" of the plate.

Quantitative analysis indicated a mean 59.0% bone fraction filling the cage in the elastically deformable group at 14 weeks compared with a mean of 44.6% in the dynamic group. This was a statistically significant difference (p=.001). At 18 weeks, the mean bone fraction of elastically deformable plate specimens was 41.2%, whereas the mean in the dynamic-plated group was 26.7%. These differences approached statistical significance (p=.125, power=65.4%, effect size 1.03, minimum detectible difference 23.1%) but were underpowered because of variation in the data at 18 weeks. When pooling the bone volume fraction for both time points, the mean bone fraction of all elastically deformable specimens (52.4%) was superior to all dynamic-plated specimens (35.7%). This difference was statistically significant (p=.019). Quantitative assessment of bone fraction is shown in Table 2.

Discussion

In this study, we used the well-established goat ACDF model. Although there are undoubtedly differences between the biomechanics of the goat and human cervical spine, loading in the cervical spine of the goat is analogous to humans [29–31]. The posture and kinematics of the head and neck of the goat are similar to humans [32] as are the musculature and bony ligamentous structures in the cervical spine [29,33–35]. The goat ACDF model has been used for more than 25 years for evaluating ACDF treatments [36–42] and is established as an excellent but challenging model for cervical fusion [32,33,43–45]. The time course of fusion is well-defined in the goat ACDF model. At the early time point of 6 weeks, only 2% of levels are expected to be fused [36], whereas at 12 weeks, the course of fusion is variable, with fusion rates ranging from 0% to 52% [32–34,36–42]. By 24 weeks, fusion rates are 33%–80%, depending on treatment [36,38], and at 12 months, fusion rates are 66%–100% [38].

The critical time points for this study were 8 and 12 weeks for CT scans and 14 and 18 weeks for histology. These time points were chosen to compare bone formation and extent of bridging bone at early time points (8 and 12 weeks) to determine if the elastically deformable plate accelerated bone formation. Bridging bony fusion as an outcome was assessed at the later time points of 14 and 18 weeks. The 18-week time point was chosen as more indicative of the final outcome (fusion vs. pseudarthrosis) for each motion segment, whereas at 14 weeks, fusion was still progressing in most animals.

Results from this preliminary study demonstrate that the elastically deformable plate which facilitates micro-motion is efficacious for achieving early bone formation, early bridging bone, and interbody fusion in the challenging goat ACDF model. The study was designed and powered with bone formation (as determined via histology) as the primary outcome measure. This quantitative objective measurement assesses the rate and quantity of bone formation in the disc space and is indicative of time course of fusion. Fusion assessment based on CT scan at the earlier time points was more subjective and more variable. Results from this preliminary study show that mean values in every assessment at all time points for the elastically deformable plate were comparable with or superior to those for the translationally dynamic plate. These results suggest that implants that facilitate load-sharing through controlled micro-motion facilitate faster bone formation and better early outcomes. However, because of variations within each treatment group, the study was underpowered, and it remains unclear whether the enhancements observed on CT scans for the elastically deformable treated levels are significantly superior to the dynamic-treated levels. Further studies will be needed to more definitively determine the long-term time course to mature fusion and to detail the advantages of the load-sharing.

The role of biomechanics and load-sharing in optimizing spine fusion surgery is not well defined. Dynamic cervical plates [20], PEEK interbody cages [46], PEEK rods (in the lumbar spine) [47], and other flexible fusion systems purport to promote load-sharing and minimize stress shielding in the spine. Biomechanically, the plate used in this study is unique in that it facilitates continuous load-sharing through elastic micro-motion. The plate is fabricated from titanium alloy (not a low stiffness polymer), which allows true elastic deformation and continuous load-sharing through the entire range of motion of the cervical spine. The elastically deformable plate allows for load-sharing at both low and high loads during

flexion, extension, and lateral bending. Results from this study suggest that the combination of continuous load-sharing and stability through the entire range of physiological loading promotes faster bone formation and better fusion.

Although outcomes are generally good clinically for single-level fusion, the advantages of load-sharing through micro-motion may be more significant for patients with comorbidities where pseudarthrosis rates are higher. This is particularly relevant for spinal fusion procedures in challenging populations such as smokers and patients with diabetes who have diminished bone formation [1,2] and reduced fusion rates [3,4]. Although the potential for load-sharing and micro-motion to augment spine fusion in smokers and in patients with diabetes has not been studied, there is evidence in the fracture fixation literature that suggests that optimal load-sharing can be an effective means of enhancing outcomes. In fracture healing, the most common factor leading to non-union is impairment of bone vascularity due to smoking and diabetes [48,49]. Micro-motion at the fracture site by flexible fixation, dynamization, or weight bearing is effective in stimulating fracture healing even in patients who are smokers and those with diabetes [48,50,51]. Fundamentally, mechanical loading enhances bone formation even in patients with diabetes and those who smoke, and thus, optimal load-sharing has the potential to improve fusion outcomes for difficult-to-treat populations [52–54].

Conclusions

Although the optimal implant stiffness is not yet characterized, results from this study demonstrate that the elastically deformable implant promoted superior early bone formation in the challenging goat ACDF model. Data also suggest that the elastically deformable implant promotes early bony bridging and rates of fusion comparable with or superior to a translationally dynamic plate, but a future study that is sufficiently powered will be needed to definitively assess the advantages of load-sharing through micro-motion. A more comprehensive understanding of these relationships may be paradigm-shifting with respect to the design of next-generation implants and other therapeutic approaches to spine fusion.

Acknowledgment

This research was funded by grant R43 AR068819-01 from NIAMS of the NIH.

References

[1] Krakauer JC, McKenna MJ, Buderer NF, et al. Bone loss and bone turnover in diabetes. Diabetes 1995;44:775–82.
[2] Rubin MR. Bone cells and bone turnover in diabetes mellitus. Curr Osteoporos Rep 2015;13:186–91.
[3] Andersen T, Christensen FB, Laursen M, et al. Smoking as a predictor of negative outcome in lumbar spinal fusion. Spine 2001;26:2623–8.
[4] Hadley MN, Reddy SV. Smoking and the human vertebral column: a review of the impact of cigarette use on vertebral bone metabolism and spinal fusion. Neurosurgery 1997;41:116–24.
[5] Costa-Rodrigues J, Reis S, Teixeira S, et al. Dose-dependent inhibitory effects of proton pump inhibitors on human osteoclastic and osteoblastic cell activity. FEBS J 2013;280:5052–64.
[6] Sasso RC, Ruggiero RA Jr, Reilly TM, et al. Early reconstruction failures after multilevel cervical corpectomy. Spine 2003;28:140–2.
[7] Veeravagu A, Cole T, Jiang B, et al. Revision rates and complication incidence in single-and multilevel anterior cervical discectomy and fusion procedures: an administrative database study. Spine J 2014;14:1125–31.
[8] Chamay A, Tschantz P. Mechanical influences in bone remodeling. Experimental research on Wolff's law. J Biomech 1972;5:173–80.
[9] Goodship AE, Kenwright J. The influence of induced micromovement upon the healing of experimental tibial fractures. J Bone Joint Surg Br Vol 1985;67:650–5.
[10] Goodman S, Aspenberg P. Effects of mechanical stimulation on the differentiation of hard tissues. Biomaterials 1993;14:563–9.
[11] Frost HM. A 2003 update of bone physiology and Wolff's Law for clinicians. Angle Orthod 2004;74:3–15.
[12] Skinner HB, McMahon PJ. editors. Current diagnosis & treatment in orthopedics. New York: Lange Medical Books/McGraw-Hill Medical Publishing Division; 2006.
[13] Einhorn TA, O'Keefe RJ, Buckwalter J. Orthopaedic basic science. In: Foundations of clinical practice. Rosemont, IL: American Academy of Orthopaedic Surgeons (AAOS); 2007.
[14] Steinmetz MP, Benzel EC, Apfelbaum RI. Axially dynamic implants for stabilization of the cervical spine. Neurosurgery 2006;59:ONS-378–ONS-89.
[15] Peterson J, Chlebek C, Clough A, et al. Cervical plate stiffness affects the distribution of loads and the location of the instantaneous axis of rotation of the spine in vitro. Spine J 2016;16:S260–1.
[16] Peterson J, Chlebek C, Ledet EH. Spinal fusion implant stiffness affects load sharing. Spine J 2016;16:S260.
[17] Peterson J, Chlebek C, Meier K, et al. Variable stiffness cervical plates affect load sharing in the interbody space in vitro. In: Proceedings of the 61st Annual Meeting of the Orthopaedic Research Society. Rosemont, IL: Orthopaedic Research Society; 2015. p. 1141–2.
[18] Peterson JM, Chlebek C, Clough AM, et al. Optimization of spinal fusion implant stiffness and its effect on instantaneous axis of rotation. In: Proceedings of the 2015 41st annual Northeast Biomedical Engineering Conference (NEBEC). Troy, NY: IEEE; 2015. p. 1–2. doi:10.1109/NEBEC.2015.7117121.
[19] Brodke DS, Gollogly S, Mohr RA, et al. Dynamic cervical plates: biomechanical evaluation of load sharing and stiffness. Spine 2001;26:1324–9.
[20] Brodke DS, KlimoJr P, Bachus KN, et al. Anterior cervical fixation: analysis of load-sharing and stability with use of static and dynamic plates. J Bone Joint Surg 2006;88:1566–73.
[21] Rapoff AJ, Conrad BP, Johnson WM, et al. Load sharing in Premier and Zephir anterior cervical plates. Spine 2003;28:2648–50.
[22] Haid RW, Foley KT, Rodts GE, et al. The cervical spine study group anterior cervical plate nomenclature. Neurosurg Focus 2002;12:1–6.
[23] Stulik J, Pitzen TR, Chrobok J, et al. Fusion and failure following anterior cervical plating with dynamic or rigid plates: 6 month results of a multi-centric, prospective, randomized, controlled study. Eur Spine J 2007;16:1689–94.
[24] DiAngelo DJ, Foley KT, Vossel KA, et al. Anterior cervical plating reverses load transfer through multilevel strut-grafts. Spine 2000;25:783–95.
[25] Tye GW, Graham RS, Broaddus WC, et al. Graft subsidence after instrument-assisted anterior cervical fusion. J Neurosurg Spine 2002;97:186–92.
[26] Fogel GR, Li Z, Liu W, et al. In vitro evaluation of stiffness and load sharing in a two-level corpectomy: comparison of static and dynamic cervical plates. Spine J 2010;10:417–21.
[27] Burkus JK, Foley K, Haid R, et al. Surgical Interbody Research Group: radiographic assessment of interbody fusion devices: fusion criteria for anterior lumbar interbody surgery. Neurosurg Focus 2001;10:1–9.

[28] Chung H, Hur J, Ryu K, et al. Surgical outcomes of anterior cervical fusion using demineralized bone matrix as stand-alone graft material: single arm, pilot study. Korean J Spine 2016;13:114–19.
[29] Smit TH. The use of a quadruped as an in vivo model for the study of the spine—biomechanical considerations. Eur Spine J 2002;11:137–44.
[30] Wachs R, Grabowsky M, Glennon JC, et al. In vivo loads in the cervical spine: a preliminary investigation using a force sensing implant. Spine J 2012;12:S141.
[31] Ledet EH, Peterson J, Wachs RA, et al. Direct measure of cervical interbody forces in vivo: load reversal after plating. Spine J 2016;16:S362–3.
[32] Zdeblick TA, Cooke ME, Wilson D, et al. Anterior cervical discectomy, fusion, and plating. A comparative animal study. Spine 1993;18:1974–83.
[33] Zdeblick TA, Wilson D, Cooke ME, et al. Anterior cervical discectomy and fusion. A comparison of techniques in an animal model. Spine 1992;17:S418–26.
[34] Zdeblick TA, Ghanayem AJ, Rapoff AJ, et al. Cervical interbody fusion cages. An animal model with and without bone morphogenetic protein. Spine 1998;23:758–65, discussion 66.
[35] Constantinescu G. Guide to regional ruminant anatomy based on the dissection of the goated. Ames, IA: Blackwell; 2001.
[36] Pintar FA, Maiman DJ, Hollowell JP, et al. Fusion rate and biomechanical stiffness of hydroxylapatite versus autogenous bone grafts for anterior discectomy. An in vivo animal study. Spine 1994;19:2524–8.
[37] Zdeblick TA, Cooke ME, Kunz DN, et al. Anterior cervical discectomy and fusion using a porous hydroxyapatite bone graft substitute. Spine 1994;19:2348–57.
[38] Brantigan JW, McAfee PC, Cunningham BW, et al. Interbody lumbar fusion using a carbon fiber cage implant versus allograft bone: an investigational study in the Spanish goat. Spine 1994;19:1436–43.
[39] Toth JM, An HS, Lim T-H, et al. Evaluation of porous biphasic calcium phosphate ceramics for anterior cervical interbody fusion in a caprine model. Spine 1995;20:2203–10.
[40] Mooney V, Massie JB, Lind BI, et al. Comparison of hydroxyapatite granules to autogenous bone graft in fusion cages in a goat model. Surg Neurol 1998;49:628–34.
[41] Cahill DW, Martin GJ Jr, Hajjar MV, et al. Suitability of bioresorbable cages for anterior cervical fusion. J Neurosurg Spine 2003;98:195–201.
[42] Gu Y, Zhang F, Lineaweaver WC, et al. In vivo study of hydroxyapatite-coated hat type cervical intervertebral fusion cage combined with IGF-I and TGF-β1 in the goat model. Clin Spine Surg 2016;29:E267–75.
[43] Khan SN, Lane JM. Spinal fusion surgery: animal models for tissue-engineered bone constructs. Biomaterials 2004;25:1475–85.
[44] Drespe IH, Polzhofer GK, Turner AS, et al. Animal models for spinal fusion. Spine J 2005;5:209S–16S.
[45] Alini M, Eisenstein SM, Ito K, et al. Are animal models useful for studying human disc disorders/degeneration? Eur Spine J 2008;17:2–19.
[46] Weiner BK, Fraser RD. Lumbar interbody cages. Spine 1998;23:634–40.
[47] Highsmith JM, Tumialán LM, Rodts GE Jr. Flexible rods and the case for dynamic stabilization. Neurosurg Focus 2007;22:1–5.
[48] Gaston M, Simpson A. Inhibition of fracture healing. J Bone Joint Surg 2007;89-B:1553–60.
[49] Ciuvica R, Vasilescu M, Bordianu A, et al. Our experience in treating femoral diaphyseal fractures and their most common complications. Med Sportiva 2013;9:2191–7.
[50] Litrenta J, Tornetta P, Vallier H, et al. Dynamizations and exchanges: success rates and indications. J Orthop Trauma 2015;29:569–73.
[51] Bottlang M, Fitzpatrick D, Sheerin D, et al. Dynamic fixation of distal femur fractures using far cortical locking screws: a prospective observational study. J Orthop Trauma 2014;28:181–8.
[52] Turner CH, Forwood M, Rho JY, et al. Mechanical loading thresholds for lamellar and woven bone formation. J Bone Miner Res 1994;9:87–97.
[53] Chambers TJ, Evans M, Gardner TN, et al. Induction of bone formation in rat tail vertebrae by mechanical loading. Bone Miner 1993;20:167–78.
[54] Morgan EF, Lei J. Toward clinical application and molecular understanding of the mechanobiology of bone healing. Clin Rev Bone Miner Metab 2015;13:256–65.